Available online at www.sciencedirect.com
ScienceDirect
Polymer 48 (2007) 1030–1041
polymer
www.elsevier.com/locate/polymer

New criterion for craze initiation

C.B. Bucknall*

Advanced Materials Department, Cranfield University, SIMS B61, Bedford MK43 0AL, UK

Received 10 July 2006; received in revised form 27 November 2006; accepted 17 December 2006
Available online 20 December 2006

Abstract

Existing criteria for craze initiation are reviewed, and their limitations are discussed. The most obvious problem is that they are formulated simply in terms of principal stresses, making no provision for the known effects of small inclusions and surface imperfections. To solve this problem, a new criterion is proposed, which is based on linear elastic fracture mechanics. Craze initiation is treated as a frustrated fracture process rather than a yield mechanism. Calculations show that the strain energy release rate, G_I(nasc), required to generate a typical 20 nm thick nascent craze, is less than 1 J m^{-2}. This explains why flaws less than 1 μm in length are capable of nucleating crazes at stresses of 20–30 MPa. Subsequent craze propagation is dependent upon two flow rates, one relating to fibril drawing at the craze wall and the other to shear yielding at the craze tip. Under biaxial stress, the second principal stress σ_2 affects craze tip shear yielding but not fibril drawing. This model is used in conjunction with the von Mises yield criterion to derive a new expression for the crazing stress σ_1(craze), which provides a good fit to data on visible crazes obtained by Sternstein, Ongchin and Myers in biaxial tests on cast PMMA [Sternstein SS, Ongchin L, Silverman A. Appl Polym Symp 1968;7:175; Sternstein SS, Ongchin L. Polym Prepr Am Chem Soc Div Polym Chem 1969;10:1117; Sternstein SS, Myers FA. J Macromol Sci Phys 1973;B8:539].

Keywords: Craze initiation; Craze propagation; Biaxial stress

1. Introduction

Despite more than 50 years of active research on crazing, the initiation step is still poorly understood [4,5]. By contrast, there are now well-developed theories on craze tip advance, craze thickening [6], and fibril failure. Building upon Argon and Salama's meniscus instability criterion for craze propagation [7], Kramer showed how resistance to craze propagation increases with entanglement density, and is therefore dependent on chain length and molecular characteristics [8]. At about the same time, Lauterwasser and Kramer showed that crazes thicken by a cold drawing mechanism, in which existing fibrils pull fresh material from the craze walls [9]. This work led to an understanding of the role of entanglements in determining the natural draw ratio λ_{craze} for fibrils [10], and later to quantitative models for craze failure, involving chain rupture and disentanglement by forced reptation [11,12]. Each of these topics now has a firm foundation in polymer physics, enabling them to be investigated and developed theoretically at the molecular level [13–18].

The same cannot be said about craze initiation. Criteria proposed more than 30 years ago by Sternstein and Ongchin [1,2], and later by Oxborough and Bowden [19], provide good fits to the experimental data, but leave a number of important questions unanswered. They assume that crazing is simply a distinctive type of yielding, and are therefore formulated to resemble standard yield criteria. Unfortunately they are perceived as being more difficult to apply [4,5]. Before discussing the reasons for these difficulties, it is instructive to review the criteria for ordinary plastic deformation (shear yielding), with which craze criteria are regularly compared.

* Tel.: +44 (0) 1234 750 421.
E-mail addresses: clivebucknall@aol.com; c.b.bucknall@cranfield.ac.uk

0032-3861/$ - see front matter © 2007 Elsevier Ltd. All rights reserved.
doi:10.1016/j.polymer.2006.12.033

2. Shear yielding

Various criteria have been proposed to define conditions for yielding in ductile materials, the best known being those due to Tresca, Coulomb and von Mises. They are based purely upon the applied stress, and make no allowance for time-dependence. At low stresses, the time-dependent deformation behaviour of polymers is well described by linear viscoelasticity theory, but at higher stresses it is better represented by the Eyring flow equation [20,21]:

$$\dot{\varepsilon} = \dot{\varepsilon}_0 \exp - \left(\frac{\Delta G - \tau_{\mathrm{oct}} V - \sigma_{\mathrm{m}} \Omega}{k_{\mathrm{B}} T} \right) \tag{1}$$

where $\dot{\varepsilon}$ = flow rate, ΔG = activation free energy, V = shear activation volume, Ω = dilatation activation volume, k_{B} = Boltzmann's constant, T = temperature; τ_{oct} and σ_{m} are the octahedral shear stress and the mean normal stress (isotropic component of the stress tensor, also known as negative pressure or hydrostatic tension) given, respectively, by:

$$\tau_{\mathrm{oct}} = \frac{\left[(\sigma_1 - \sigma_2)^2 + (\sigma_2 - \sigma_3)^2 + (\sigma_3 - \sigma_1)^2 \right]^{1/2}}{3} \tag{2}$$

$$\sigma_{\mathrm{m}} = \frac{\sigma_1 + \sigma_2 + \sigma_3}{3} \tag{3}$$

where σ_1, σ_2 and σ_3 are the three principal stresses. The von Mises yield criterion specifies that yielding occurs when τ_{oct} reaches a critical value. Alternatively, the criterion can be expressed in terms of a critical effective stress, σ_{e}, as follows:

$$\sigma_{\mathrm{e}} = \frac{3\tau_{\mathrm{oct}}}{\sqrt{2}} = \left[\frac{(\sigma_1 - \sigma_2)^2 + (\sigma_2 - \sigma_3)^2 + (\sigma_3 - \sigma_1)^2}{2} \right]^{1/2} = \sigma_{\mathrm{y}} \tag{4}$$

where σ_{y} is the shear yield stress in both uniaxial tension and uniaxial compression. As implied by Eq. (1), σ_{y} is a function of strain rate and temperature. In polymers, the critical value of σ_{e} at yield is a function of σ_{m}, which means that the yield stress is lower in tension than it is in compression. It is therefore necessary to modify the von Mises equation by adding an extra term, as follows [2,3,20,21]:

$$\sigma_{\mathrm{e}} + \mu \sigma_{\mathrm{m}} = \sigma_{\mathrm{crit}} \quad \text{at yield} \tag{5}$$

where μ is a pressure coefficient (typically $\sim$0.38).

Under certain conditions, for example in tensile tests at 23 °C on polycarbonate (PC), the flow rate can increase sufficiently to match the applied strain rate, so that the specimen reaches a maximum load, necks, and draws before there is any observable crazing. In that sense, PC can be said to be craze resistant. On the other hand, crazes form readily in PC at the tips of sharp notches, for example in fracture mechanics tests where the material experiences plane strain deformation. Under these conditions, crazing is both the first stage of brittle fracture and a mechanism of yielding that can be modelled using the Dugdale line zone analysis [22]. The dual nature of crazing appears to be one of the main reasons why there have been so many problems in formulating a satisfactory criterion for craze initiation.

3. Criteria for craze initiation

Crazes are crack-like deformation zones formed on planes normal to the direction of maximum (tensile) principal stress [1]. Load-bearing fibrils connect the walls of the craze. In homogeneous glassy polymers such as polystyrene (PS) and poly(methyl methacrylate) (PMMA), crazes are usually initiated from microscopic surface flaws or embedded dust particles. Dust is difficult to avoid in injection moulding or extrusion, because these processes begin with pellets that become statically charged and attract airborne particles. Cast PMMA, which is made directly from the monomer, is usually much less contaminated.

Typical surface marks are small random scratches introduced during processing, machining and handling. When these flaws are removed by assiduous polishing, there is a marked increase in σ_1(craze), the critical stress for crazing, sometimes to the point at which tensile shear yielding and ductile drawing are produced in relatively brittle polymers such as PMMA and PS [23]. Similarly, shear yielding can be generated in PMMA by using a very low strain rate, so that the yield stress is reduced as predicted by Eq. (1) [3].

Thus any reproducibility obtained in crazing tests on well-prepared un-notched specimens appears to depend upon the presence of a characteristic population of microscopic surface flaws or embedded foreign particles. This is certainly true for high-impact polystyrene (HIPS), where rubber particles with diameters of 1–5 μm initiate crazes in such profusion that yielding occurs with very little assistance from shear deformation [24]. The importance of flaws and heterogeneities is widely recognized, and is discussed at length in papers by Sternstein and Rosenthal [25] and Argon [26]. Nevertheless, the problem of how to account quantitatively for the effects of these flaws has never been properly resolved. There has been some discussion on flaw shape and its effect on local stress concentrations [26], but questions relating to flaw size have been almost entirely neglected.

The earliest studies of craze formation were carried out in uniaxial tension. Maxwell and Rahm used creep tests on polystyrene to show that rates of crazing increase rapidly with applied stress and temperature [27]. Subsequent analysis has demonstrated that these kinetic data can be correlated using the Eyring equation [24]. Because of the exponential dependence of rate upon applied stress, it is possible to define a critical tensile stress for craze formation occurring within a set time period. Since the introduction of the Bergen elliptical strain jig [28], it has been more convenient to specify a critical tensile strain for crazing, especially in studies of 'solvent' crazing.

To investigate crazing under multi-axial loading, Sternstein et al. cut circular holes through the thickness of PMMA plates, and subjected them to uniaxial tensile stress [1]. In later work

on the same grade of PMMA, Sternstein and Ongchin applied internal pressure plus axial tension to thin-walled cylinders [2], and Sternstein and Myers subjected cylindrical rods to combined tension and torsion [3]. These investigators were thus able to observe craze formation in PMMA under various states of biaxial loading, encompassing both tension–tension [2] and tension–compression [3]. They demonstrated that there is a boundary between stresses that produce visible crazes, and those that do not. On the basis of these observations, they proposed the following criterion for craze formation:

$$\sigma_b = |\sigma_1 - \sigma_2| = A(T) + \frac{B(T)}{\sigma_1 + \sigma_2 + \sigma_3} \quad (6)$$

where σ_b is termed the 'stress bias', and the quantities $A(T)$ and $B(T)$ are materials constants at fixed temperature T.

For the case of biaxial loading, Eq. (6) gives a good fit to the experimental data in both the first (tension–tension) and second (tension–compression) quadrants of principal stress space, as demonstrated in Fig. 1. The stress-bias curve defines the lower bound for craze formation. No crazing is observed at lower applied stresses [3]. Fig. 2 is a more general overview comparing the stress-bias curve, Eq. (6), with the pressure-modified von Mises yield criterion Eq. (5). This comparison was first made by Sternstein and Ongchin [2], who clearly regarded crazing as an alternative plastic deformation mechanism, which they termed 'normal stress yielding'.

The stress-bias criterion has not met with universal acceptance. The main criticisms have been:

(a) Although Eq. (6) is described as a critical stress-bias criterion, crazing is observed even when $\sigma_1 \approx \sigma_2$ and $\sigma_b \approx 0$. In view of this observation, it is obvious that σ_b is not the driving stress for craze initiation. If Eq. (6) is to be retained, it would be more logical to invert it, and define a critical mean stress that is dependent upon σ_b. A better name might be the (stress-bias dependent) critical mean stress criterion.

(b) The magnitude of the stress bias is twice the shear stress on planes at 45° to the 1 and 2 axes. This again suggests that σ_b has no direct bearing on craze thickening, which produces a displacement along the 1 axis, a further indication at the major principal stress, σ_1, is the main driver of craze initiation. This view is supported by the observations that there is no preferred orientation for the craze planes when $\sigma_1 = \sigma_2$, and that these planes are normal to σ_2 when $\sigma_2 > \sigma_1$ [29].

(c) The reasons for defining the stress bias simply as $|\sigma_1 - \sigma_2|$ are unclear. When σ_2 is positive and $\sigma_3 = 0$, $|\sigma_1 - \sigma_3|$ is larger than $|\sigma_1 - \sigma_2|$ but is not included in the criterion. It is difficult to understand why one stress-bias term is critical while another has no effect.

(d) The physical principles responsible for the inverse dependence upon the hydrostatic tension are unclear, an issue that continues to attract adverse comment [17].

(e) Since the maximum stress concentration factor is only ~2 near to a spherical void or rubber particle, it is not obvious why very small holes or particles are such effective craze initiators.

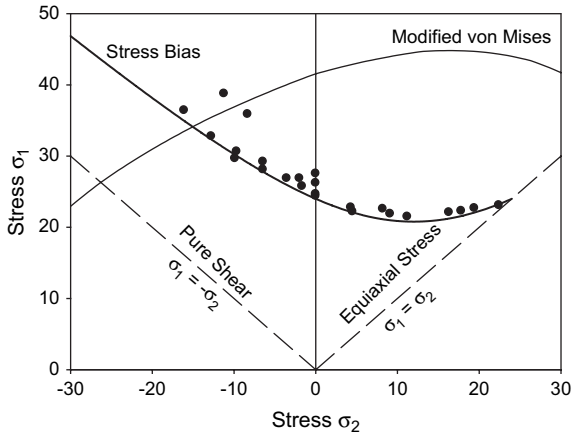

Fig. 1. The stress-bias criterion, Eq. (6), which defines the lower bound for craze formation under biaxial loading, with experimental data on visible crazing in cast PMMA at 60 °C. The mean stress is zero under pure shear, where $\sigma_1 = -\sigma_2$. The diagram is symmetrical about the equiaxial stress line $\sigma_1 = \sigma_2$. (After Sternstein et al. [2,3].)

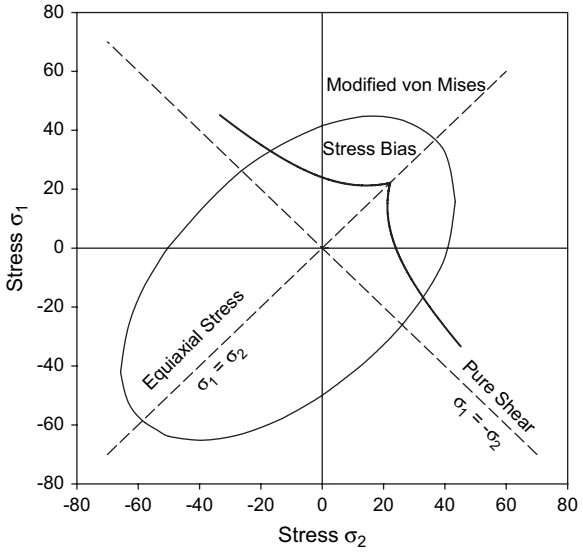

Fig. 2. Overview of stress-bias criterion, Eq. (6), in biaxial stress space, with pressure-modified von Mises yield criterion, Eq. (5), for PMMA at 60 °C. (After Sternstein and Ongchin [2].)

Some reviewers have also expressed reservations about the stress-bias criterion on the grounds that it is difficult to apply, because it requires knowledge of local stress states close to the origin of each individual craze, and that is usually lacking in the case of small flaws [4,5,30,31]. Sternstein himself attributes crazing under equal biaxial stress to local anisotropy in the stress state due to adventitious flaws and structural fluctuations [29]. These comments raise some interesting questions about craze initiation criteria. If the critical local stresses σ_{1L}(craze) and σ_{2L}(craze) close to flaws are not directly and systematically related to the macroscopic applied

stresses, how is it possible to obtain well-correlated and reproducible data for the relationship between $\sigma_{1\infty}$(craze) and $\sigma_{2\infty}$(craze), the applied principal stresses at craze initiation? The subscripts L and ∞ are used here to distinguish local from global stresses.

In an effort to develop a criterion based on more logical physical principles, Oxborough and Bowden proposed the following critical tensile stress criterion [19]:

$$\sigma_1 - \nu(\sigma_2 + \sigma_3) = C(t,T) - \frac{D(t,T)}{\sigma_1 + \sigma_2 + \sigma_3} \tag{7}$$

which they converted into a critical tensile strain criterion, as follows:

$$\varepsilon_1 = \frac{1}{E}\left[C(t,T) - \frac{D(t,T)}{\sigma_1 + \sigma_2 + \sigma_3}\right] \tag{8}$$

These equations overcome some of the problems listed above, but are still essentially revised versions of Sternstein and Ongchin's stress-bias criterion. Not only do they preserve the term in reciprocal pressure, but also they are not firmly based on *a priori* physical principles, and are open to the same criticism, i.e. they are difficult to apply because they require a knowledge of local stress states near microscopic flaws.

Argon and Hannoosh have carried out a comprehensive theoretical evaluation and experimental evaluation of the stress-bias criterion [23]. Their model for craze initiation assumes that individual voids are nucleated in regions of high stress concentration, which are usually close to scratches, embedded dust or rubber particles. They recognize that it is exceedingly difficult to nucleate closed pores in a continuous homogeneous material, because that requires hydrostatic tensions approaching the theoretical cohesive strength of the material. As craze stresses are usually below $\sigma_y/3$, improbably high stress concentrations would be required to form pores in this way [23,32]. To overcome this problem, they proposed a mechanism of microcracking in which the arrest of micro-shear bands is the first step in pore nucleation, a concept that has its origins in crystal plasticity [33].

The applicability of this pore nucleation mechanism to glassy polymers is questionable. Closed pores are known to form in rubber-toughened polymers, where cavitation of the rubber particles is an integral part of the toughening mechanism, but the energy barriers to void nucleation are high, especially when the shear modulus of the rubber phase is above 1 MPa [34–38]. Lightly cross-linked elastomers exhibit moduli below 1 MPa at temperatures well above T_g, but exceptional conditions would be needed to nucleate an internal void in a glassy polymer at cryogenic temperatures, where crazing is regularly observed.

Relatively soon after proposing their closed-pore model, Argon and Hannoosh recognized that it cannot be applied to craze propagation [23]. There are two problems: it fails by orders of magnitude to account for the observed rates of craze growth, and it predicts the formation of a closed-cell foam, which could not give rise to the fibrillar open structure of a craze. As an alternative, they proposed the meniscus instability criterion illustrated in Figs. 3 and 4. This begins with a typical concave air–polymer interface (the meniscus), which is usually represented as the rounded tip of an existing craze. The liquid-like meniscus adopts a shape that minimizes surface energy, in accordance with standard theory. Ahead in the propagation direction is a void-free plastic zone. A plan view shows all points along the advancing meniscus initially lying approximately on a straight line or smooth curve. However, the small surface area of the meniscus limits the rate of flow in the fluid zone, and therefore the rate at which the flow front advances. Consequently, the meniscus becomes unstable when the solid blocks of polymer enclosing the meniscus are pulled apart at a sufficiently high rate. Instead of maintaining a linear flow front, the interface extends air-filled fingers forward into the fluid zone. In other words, it breaks. Examples of this behaviour, on a much larger scale, have been observed in layers of rubber bonded between rigid plates that are pulled apart at a constant rate [39]. In crazes, the oriented walls that

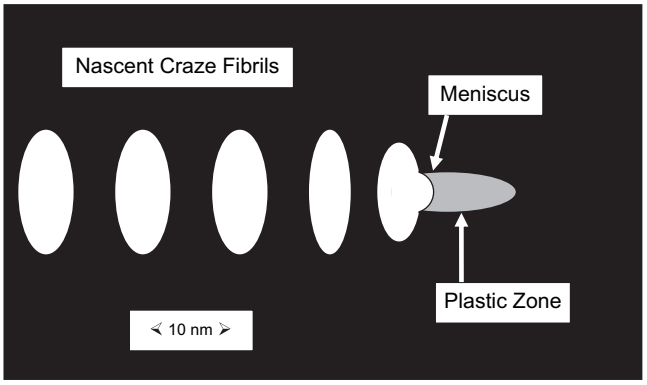

Fig. 3. Schematic profile view of craze tip showing nascent fibrils ~6 nm in diameter, and plastic zone with fluid meniscus.

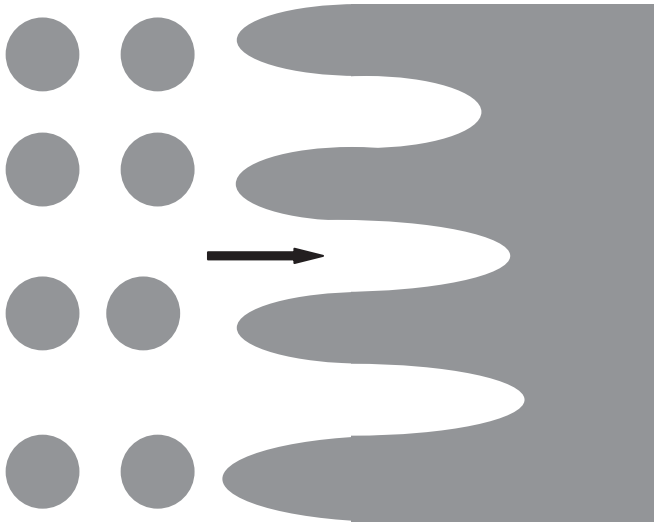

Fig. 4. Schematic plan view of craze tip, showing air fingers extending into the plastic zone, leaving craze fibrils in their wake. Arrow indicates propagation direction.

separate neighbouring air-filled fingers eventually break up, leaving the characteristic fibrillar structure.

The meniscus instability mechanism overcomes the problems posed by the pore nucleation model for craze propagation. It is not necessary to rely on special effects to account for hypothetical pore formation. The meniscus simply advances like a sharp transverse crack propagating through an aligned fibre composite, leaving load-bearing fibrous material in its wake. However, despite the success of this model, both Argon and Kramer retained the pore nucleation principle to explain craze initiation [26,31,32]. Their main reason for doing so appears to be that it offers an explanation for the dependence of σ_1(craze) on hydrostatic stress and shear stress, as expressed by the stress-bias criterion and its successors.

There are two major problems associated with this approach. First, it is difficult to understand why two completely different mechanisms should be needed for the same physical process, which produces a fibrillated craze. Second, as already conceded by its originators, the pore model results in a closed-cell foam, which is most unlikely to produce a craze-generating open meniscus. The obvious solution is to discard the closed-pore hypothesis, and rely entirely on the meniscus instability mechanism to explain both initiation and propagation.

Finally it should be noted that Kausch, in a review dated 1983, includes linear elastic fracture mechanics (LEFM) as a possible basis for a craze initiation criterion, citing papers on solvent crazing [30]. There is some logic behind this proposal, in that crazes always extend ahead of propagating cracks in rigid glassy thermoplastics. However, it has subsequently received little attention or support from the polymer mechanics community, essentially because it produces unrealistic values for the fracture energy G_{IC} at craze initiation when measured or estimated values of flaw size a_0 and applied stress σ_1(craze) are inserted into the Griffith equation [40]:

$$\sigma_1(\text{crit}) = \left[\frac{EG_{IC}}{Y^2(1-\nu^2)\pi a_0}\right]^{1/2} \tag{9}$$

where E = Young's modulus, ν = Poisson's ratio, and Y is a geometrical factor.

As noted earlier, crazes form in apparently flawless PMMA and PS specimens at tensile stresses of 20–40 MPa. Closer inspection reveals that flaws are present, but have very small dimensions. For example, Argon and Hannoosh observed craze initiation in PS from rounded blunt scratches up to ~0.25 μm deep. Dust particles with diameters of ~1 μm are equally capable of initiating crazes, and rubber particles with diameters of 1 μm are also extremely effective [24].

The limitations of LEFM in predicting craze initiation were first noted by Berry, who measured the critical tensile strengths σ_c of polystyrene bars containing introduced edge cracks [41]. For cracks with lengths $a_0 \geq 1$ mm, σ_c^2 varied linearly with $1/a_0$, in accordance with Eq. (9). However, when the cracks were below 1 mm in length, fracture did not occur from the introduced crack. Instead, brittle failure was initiated from previously undetected imperfections located elsewhere on the surface of the bar. Consequently σ_c became independent of a_0, remaining constant at ~40 MPa. Thus microscopic barely visible flaws proved to be more potent initiators of crazes and cracks than clearly visible 1 mm introduced cracks. In the face of this evidence, it was difficult to see how LEFM could be applied successfully to craze initiation. The evident absence of 1 mm crack-like defects, which would be easy to see in a transparent glassy polymer like polystyrene, led Drabble et al. to dismiss the fracture mechanics approach, and develop a model for internal void formation within the solid polymer as an alternative mechanism of craze initiation [42]. As noted earlier, this closed-pore model has since been discredited [26].

The foregoing review identifies a number of difficulties and inconsistencies in existing theories of craze initiation, which are unlikely to be resolved without a paradigmatic shift in thinking. The aim of the present paper is to develop a new criterion for craze initiation that addresses these problems. To be worthwhile, the model should offer an insight into the fundamental mechanisms of craze initiation, and enable researchers to develop the subject theoretically, so that craze initiation becomes properly integrated into polymer physics.

4. New criterion for craze initiation

Before attempting to formulate a new criterion, it is first necessary to define what is meant by the term 'craze initiation'. Here, the evidence provided by transmission electron microscopy (TEM) is particularly valuable. Studies on craze tips in PMMA and PS show that the minimum thickness of a newly formed craze layer is between 12 and 20 nm [31,43]. Since $\lambda_{craze} = 4.3$ in PS [10], the solid layer that produces a nascent craze in this polymer cannot be more than 5 nm thick. For PMMA, in which $\lambda_{craze} = 2.6$, the calculated initial thickness is about 8 nm.

Through the mechanism of fibril drawing, newly formed crazes can increase in thickness by a factor of more than 100. Optical interferometry shows that they eventually reach thicknesses of ~3 μm in PMMA before fracture [44], and Lauterwasser and Kramer have recorded a 7 μm thick craze at a crack tip in PS [9]. On the basis of this evidence, it is clear that G_I(craze), the energy required to initiate unit area of a nascent craze which is only 0.02 μm thick, is much smaller than the G_{IC} values measured in conventional LEFM tests, and that the case for dismissing the fracture mechanics approach to craze initiation is not as strong as it has appeared to be in the past. The TEM studies also show that crazes cannot become visible to the naked eye until they have grown considerably in thickness and in length. The amount of white light reflected from a 20 nm thick layer is negligible, and crazes with lengths below 10 μm are very hard to see. To achieve the necessary growth, the local applied stress must reach σ_{fd}, the nominal fibril drawing stress, which is a function of the shear yield stress σ_y and the strain rate [5,31].

Further relevant evidence is presented in Fig. 5. The data come from LEFM tests on PS and PMMA samples of differing viscosity average molecular weights M_v [45,46]. Because molecular weight is an unsatisfactory basis for comparing two different polymers, the measured fracture toughness G_{IC} has

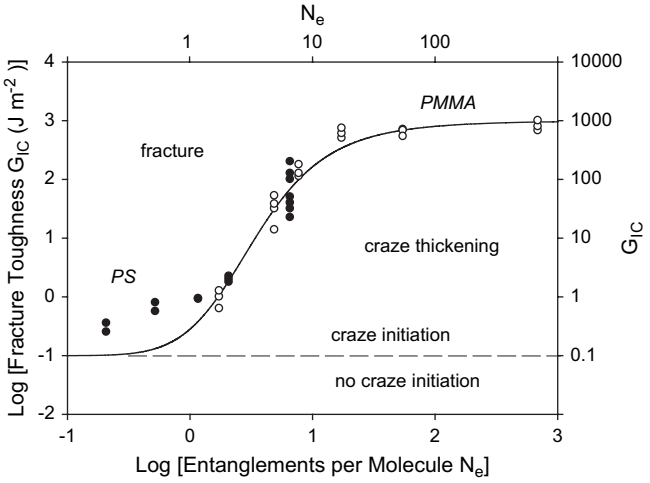

Fig. 5. Log–log relationship between fracture toughness G_{IC} and N_e, the average number of entanglements per chain, calculated as M_v/M_e, where M_v and M_e are the viscosity average and entanglement molecular weights, respectively. (●) data on PS from Ref. [45]; (○) data on PMMA, from Ref. [46].

been plotted against N_e, the average number of entanglements per chain. Here, $N_e = M_v/M_e$, where M_e is the entanglement molecular weight obtained from observations of the plateau region in the melt state. Following Donald and Kramer, M_e is taken as 19,100 for PS and 9150 for PMMA [10].

The van der Waals surface energy Γ_s is $\sim$40 mJ m^{-2} for PS and PMMA [8,47,48] and the minimum possible value for G_{IC} is therefore $\sim$80 mJ m^{-2}. Interestingly, the lowest data point for PS occurs at $G_{IC} = 250$ mJ m^{-2}, close to the absolute minimum, and the trend in the PMMA data is also towards this limit. In view of this, the value of 250 mJ m^{-2} obtained earlier by applying the Griffith equation to craze initiation from small spherical flaws looks more realistic. As the molecular weight of the polymer increases, entanglements come increasingly into play. Consequently, failure of crazes is flow-controlled, and G_{IC} rises steeply before levelling out at between 600 and 1000 J m^{-2}. In the third region of the graph, where G_{IC} becomes independent of M_v, chain scission is the rate controlling factor in craze failure.

The picture that emerges from this analysis is that craze initiation becomes possible when the strain energy release rate G_I is between 0.1 and 1.0 J m^{-2}, and in short-term tests on typical glassy thermoplastics is followed by a large increase in energy absorption as the craze thickens through the plastic process of fibril drawing. This view is supported by the observations of Berger on thin films stretched in situ on the stage of a TEM [11]. He found that the strains at which crazes initiate are independent of molecular weight between M_e and $100M_e$, while the extent of subsequent drawing increases rapidly with molecular weight, before reaching a plateau. In PS, initiation occurs at a strain of $\sim$0.5%, with the local failure strain eventually reaching $\sim$30%.

In view of this body of evidence, there are good reasons for looking again at the possibility of formulating a craze initiation criterion based on linear elastic fracture mechanics. Although true fracture does not immediately follow craze initiation (unless the chains are exceptionally short), it is nevertheless possible to characterize initiation in terms of a critical energy release rate, here denoted by the symbol G_I(nasc). The new criterion is then given by a modified version of the Griffith equation, as follows:

$$\sigma_1(\text{nasc}) \geq \left[\frac{EG_I(\text{nasc})}{Y^2(1-\nu^2)\pi a_0}\right]^{1/2} \tag{10}$$

The justification for applying a fracture mechanics criterion to craze initiation is that the notch-tip meniscus is unstable from the instant that fingers begin to extend forward until the nascent craze fibrils are fully stretched. There is a large and rapid increase in the extension ratio λ_1, for example from <1.2 to >4, with no intermediate position of stability. A good analogy for craze initiation and subsequent fibril drawing would be a rock climber losing his hold, falling until the safety rope is taut, then being lowered to a ledge below. The mechanics of the fall is not affected by the presence of the climbing rope, although the final outcome is. The only difference between a nascent craze in a high molecular weight polymer and a nascent crack in a very low molecular weight polymer is that in the first material the tie molecules are long enough to prevent final fracture. The criterion for instability is the same in both cases. The strain energy released when the tensile stress on the meniscus drops sharply and the walls of the flaw move apart is sufficient to supply the energy required for the newly created cohesive failure surface.

This analysis demonstrates that craze initiation should be classified as a type of brittle fracture, which is prevented from causing a complete break only by the delayed intervention of an internal reinforcement mechanism. The effectiveness of that mechanism is reduced by reducing the chain length, either at the manufacturing stage or through later degradation. The only alternative to accepting the LEFM model appears to be a return to the problems thrown up by previous craze criteria, which simply ignore the overwhelming importance of flaw size. To summarise, the arguments for the new model are as follows:

(a) Like crack growth, craze initiation is a form of cohesive failure. It is not a simple yield mechanism.
(b) The stress required to initiate crazes from microscopic flaws is a strong function of the flaw size. Careful polishing to reduce the maximum flaw size results in a substantial increase in σ_I(craze), sometimes leading to complete suppression of craze formation. This type of behaviour is characteristic of fracture processes, and is best described using equations based on fracture mechanics. Previous attempts to formulate crazing criteria without reference to flaw sizes have failed.
(c) At the onset of meniscus instability, it is impossible to determine whether the mechanism that takes place will lead to complete fracture (when chains are very short) or to craze formation (when chains are long). The same criteria apply to the initiation mechanism in both cases, although

the final outcomes are different in one important respect: there are no tensile stresses acting on the faces of a true crack, whereas a craze continues to support tensile stresses as it propagates.

(d) Energy is required to form new surface within a craze as it extends its planar area, just as in true fracture.

In this context, it is important to remember that the quantity measured in standard LEFM tests is the energy release rate G_I at instability. The only basic difference between G_{IC} and the proposed new quantity G_I(nasc) is that attainment of G_{IC} results in an increase in true crack length and therefore a further increase in G_I. Initiation of a true crack is followed immediately by crack propagation, which in standard test specimens leads to catastrophic fracture. More subtle and elaborate methods are needed to observe the initiation of a craze. Crazes should be treated as frustrated cracks, in which the walls are connected by load-bearing fibrils. There is an obvious parallel with two-stage fracture in long-fibre composites. In both cases, the brittle matrix breaks, but fibre pull-out is needed to produce complete failure.

Crazing is a cohesive failure process occurring on planes lying normal to the major principal stress. It is sometimes associated with obvious notches and precracks, but in many instances it initiates from microscopic surface flaws, at very low strain energy release rates. When the initiating flaws are large, fracture follows almost immediately. When they are very small, there is a long period of development before catastrophic brittle fracture terminates the process. This sequence of events typically takes place at stresses well below the shear yield stress.

The above statement is equally valid if the word 'crazing' is replaced with the phrase 'sub-critical crack growth', a term that embraces both dynamic fatigue and time-dependent crack growth under static loading [40]. Furthermore, at the point of instability a micron-sized observer placed close to the flaw tip would find difficulty in distinguishing between: (a) initiation of a dynamic fatigue crack during the first loading cycle; (b) initiation of sub-critical crack growth under static loading; and (c) initiation of a craze. In each of these cases, initiation is preceded by local shear yielding, albeit on a very small scale. Then, at the critical point, the yield zone becomes unstable and the crack front advances by a small (sometimes imperceptible) amount. For example, fatigue cracks in polymers advance at rates as low as 1 nm per cycle [40]. The crack does not necessarily advance uniformly across the whole front, like a line of soldiers on parade. There will almost certainly be some irregularity. If the newly formed precrack extension is temporarily held together by reinforcing fibrils, it is a craze. If not, it is a true crack. Differences between the growth behaviour of crazes and cracks are not to be found in the criteria for initiation but in the criteria for propagation.

It is worth noting that the energy release rate principle is not unique to fracture and craze initiation. It applies whenever a new surface is created in a liquid or solid. Examples include crystallization from pure liquids and solutions, and bubble formation in a pure liquid at its boiling point. The initial nucleation step is always a problem, because the energy release rates are proportional to r^3, where r is the characteristic dimension of the newly formed phase (e.g. the bubble radius), whereas the energy required to form the surface is proportional to r^2. At small r, the surface term dominates, and the energy release rate might be insufficient to overcome the energy barrier. Therefore nucleation agents such as seed crystals or beaker walls play an important part in initiating the formation of a new phase.

In his seminal work on fracture mechanics, Griffith assumed that brittle fracture initiated from atomically sharp micro-cracks, and that the stresses at the crack tips were high enough to break inter-atomic bonds. It is now recognized that crack propagation is always preceded by energy-dissipating flow around the notch tip, and fracture mechanics specimens are therefore designed to minimize that flow, by making the tip radius as small as possible and ensuring that the notch length and specimen dimensions are large enough to produce plane strain conditions. These precautions ensure that the work done in breaking through the notch-tip plastic zone is minimized, so that the measurements generate valid G_{IC} data. The same principles apply to craze initiation.

Since craze tip thicknesses are between 10 and 20 nm, the critical craze tip opening displacement δ_{craze} is smaller, typically between 6 and 15 nm, depending on the characteristic craze extension ratio λ_{craze}. Using these figures, it is possible to estimate a minimum value for G_I(nasc) in the same way that G_{IC} is estimated from the crack-tip opening displacement:

$$G_I(\text{nasc}) = \sigma_y \delta_{craze} \tag{11}$$

With $\sigma_y = 40$ MPa and $\delta_{craze} = 15$ nm, Eq. (11) gives $G_I(\text{nasc}) = 600$ mJ m^{-2}. Some of this energy is absorbed in creating new surface and stretching the material into fibrillar form; the remainder is converted into heat. The balance between surface energy and viscous work in fibril drawing is discussed in detail in a review by Kramer [31].

Using a simple model, it is possible to estimate the energy absorbed in creating new surface by forming fibrils in a specific glassy polymer. Consider a cylindrical element of solid polymer with cross-sectional area A_0 and thickness h_0, which stretches to form a cylindrical craze fibril of radius r, cross-sectional area A, and length h. The extension ratio of the fibril is given by $\lambda = h/h_0$. Assuming that stretching occurs at constant volume:

$$A = \pi r^2 = \frac{A_0 h_0}{h} = \frac{A_0}{\lambda} \tag{12}$$

Since a craze has two walls, the area of new surface, A_{sf} is given by:

$$A_{sf} = 2(A_0 - A) + 2\pi r h = 2A_0\left(1 - \frac{1}{\lambda} + \frac{h}{r\lambda}\right) \tag{13}$$

The contribution of surface energy to G_I(nasc) is then given by:

$$U_{sf} = 2\Gamma_s\left(1 - \frac{1}{\lambda} + \frac{h}{r\lambda}\right) \quad (14)$$

where Γ_s is the surface energy of the polymer forming the craze fibrils.

Typical fibril radii are ~3 nm in polystyrene [5]. With $\Gamma_s = 40$ mJ m^{-2}, $h = 12$ nm, and $\lambda = 4.3$, Eq. (14) gives $U_{sf} = 136$ mJ m^{-2}.

Thus Eq. (10) defines a new criterion for craze initiation, while Eqs. (11) and (14) illustrate the way in which the criterion can be related to craze dimensions and materials characteristics. These three equations enable craze initiation from visible cracks to be understood and predicted. With minor modifications, they are applicable to propagation from an existing craze tip. The main requirement is to adjust the strain energy release rate to allow for the closure stresses imposed by the fibrils on the craze walls, and the wedge-opening effect of the large tensile strain in the craze [22]. The application of these equations to specimens containing no obvious flaws or cracks is a greater challenge, which is addressed in Section 5.

5. Crazing from microscopic flaws

The best documented information about surface flaws comes from work by Argon and Hannoosh on crazing in polystyrene, which demonstrates that surface roughness strongly affects the kinetics of craze nucleation [23]. These authors used precision machining of annealed compression-moulded blocks to manufacture tubular specimens with a central, thin-walled hour-glass section, and polished both inner and outer surfaces of the tubes very carefully to produce a finish with no features detectable under an optical microscope. Before polishing, they observed extensive crazing in these specimens at tensile stresses of ~20 MPa. After polishing, they found that the critical stress for craze formation was raised substantially, generally to a range between 60 MPa and the shear yield stress at ~100 MPa. The next step was to introduce parallel shallow scratches by spinning the specimens about their long axes and touching the polished surfaces for 10 s with a wet velvet cloth carrying 4 μm SiC particles. After making high-resolution metal replicas, they measured the profiles of these scratches using an interference microscope, which showed that the scratches were rounded shallow grooves up to 0.25 μm deep, many of them having a semicircular cross-section. To calculate the stress concentration factor γ, they treated the grooves as being semi-elliptical in section with axes of lengths a and b, where a is the depth of the groove. Then:

$$\gamma = 1 + \frac{2a}{b} \quad (15)$$

Calculated values of γ ranged from 2.5 to 5.0.

Under applied biaxial stresses, these flaws generated very large numbers of small crazes, at surface populations rising to 100,000 cm^{-2}. This figure should be compared with populations of 10,000 cm^{-2} generated under similar applied stresses in specimens that were neither polished nor deliberately scratched. Argon et al. [32] note that Sternstein's definition of craze initiation also appears to be based on a craze density of 10,000 cm^{-2}.

On the basis of these results it is reasonable to assume that the adventitious surface damage incurred by mechanical test specimens also consists largely of shallow scratches, with depths and profiles comparable to those produced by the SiC abrasive. Applying this assumption to Sternstein's biaxial tests on PMMA at 60 °C, with $Y = 1.12$ for an edge notch [40,49,50], the values required for LEFM calculations are $E = 2$ GPa, $a_0 = 0.25$ μm, $Y^2 = 1.25$ and $\nu = 0.4$. For the lowest point on the stress-bias curve, at σ_1(craze) = 21 MPa, Eq. (10) gives G_I(nasc) = 180 mJ m^{-2}. This is probably an overestimate, because the critical stresses recorded in Fig. 1 are not necessarily craze initiation stresses. At initiation, crazes are not thick enough to reflect visible light, which requires thicknesses of at least 200 nm (i.e., half the wavelength of violet light). Consequently, the data points in Fig. 1 should be regarded as evidence for craze thickening and propagation rather than of craze initiation. Under some circumstances, these processes might occur in quick succession, but there could be a long delay.

As illustrated in Figs. 3 and 4, craze growth involves a sequence of three distinct processes: the development of a small plastic zone at the craze tip; unstable plastic flow in the meniscus leading to the formation of fingers and fibrils; and fibril drawing from the craze walls. Of these, the first two are likely to be the most susceptible to the biaxial stress state; there is no obvious reason why fibril drawing stresses σ_{fd} should be affected by the second principal stress σ_2. On the other hand there are good grounds for concluding that biaxial loading affects the behaviour of the craze tip plastic zone.

A first step towards testing this hypothesis is to simplify Eq. (4) by setting $\sigma_3 = 0$. This gives the von Mises equation under biaxial loading as:

$$\sigma_e(\sigma_1, \sigma_2) = \left(\sigma_1^2 - \sigma_1\sigma_2 + \sigma_2^2\right)^{0.5} = \sigma_{crit} - \mu\sigma_m \quad (16)$$

When $\mu = 0$ and σ_e is held constant at σ_y, this function generates the characteristic von Mises ellipse in biaxial stress space. Alternatively, inclusion of the pressure-dependent term produces the modified ellipse shown in Figs. 1 and 2. In both cases, σ_1(von Mises) reaches a maximum in the tensile quadrant, while σ_1(craze) passes through a minimum in the same region of stress space. There appears to be some sort of inverse relationship between the two criteria. A simple method for testing this possibility is to assign a fixed value S_0 to σ_1 and calculate σ_e as a function of σ_2. Eq. (16) then gives:

$$\sigma_e(S_0, \sigma_2) = \left(S_0^2 - S_0\sigma_2 + \sigma_2^2\right)^{0.5} \equiv S_0\left(1 - R + R^2\right)^{0.5} \quad (17)$$

where $R = \sigma_2/S_0$. Fig. 6 shows the curve obtained using Eq. (17) with $S_0 = 24.4$ MPa. It bears a remarkable resemblance

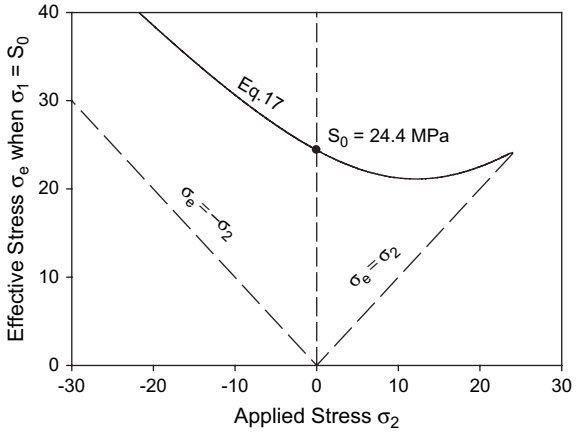

Fig. 6. Relationship between σ_2 and the corresponding effective stress $\sigma_e(S_0, \sigma_2)$, calculated using Eq. (17) with $S_0 = 24.4$ MPa.

to the stress-bias curves in Figs. 1 and 2. This observation suggests that shear plasticity exerts a controlling influence upon the formation of visible crazes. This is not surprising, since shear plasticity at the crack tip is known to control the formation of visible cracks in metal specimens which initially contain only microscopic Griffith flaws [49,50].

Further evidence in support of this conclusion is presented in Fig. 7, which compares Sternstein's biaxial data on σ_1(craze) with the local effective stress $\sigma_{eL}(S_0, \sigma_2)$ calculated using Eq. (17). It is important to emphasize that the 'local effective stress' is different from the global effective stress $\sigma_{e\infty}$ calculated for each pair of test data [σ_1(craze); σ_2(craze)]. It refers to a critical effective stress $\sigma_e(S_0, \sigma_2)$ at a specific location (yet to be identified), where the critical local stress σ_{1L} is equal to S_0, the measured critical crazing stress σ_1(craze) under uniaxial tension (in this case 24.4 MPa). The reasons for investigating this set of stresses are first that it generates the

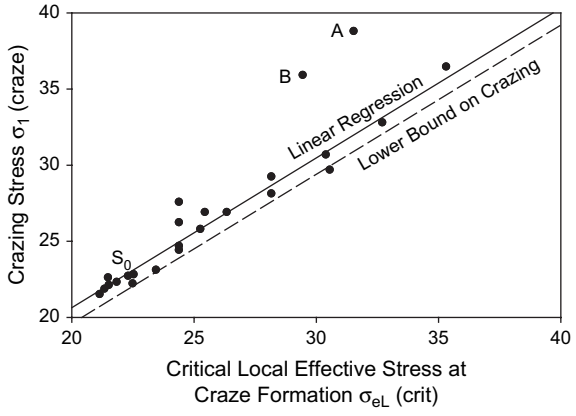

Fig. 7. Relationship between σ_1(craze) and the local effective stress $\sigma_e(S_0, \sigma_2)$, calculated using Eq. (17) by inserting $S_0 = 24.4$ MPa and $\sigma_2 = \sigma_2$(craze). Here σ_1(craze) and σ_2(craze) are the data pairs shown in Fig. 1. The (continuous) linear regression line is based on all data points except A and B, which lie well above the lower bound. The dotted line is parallel to the regression line, but passes through the origin; it marks the lower bound on the experimental data.

curve shown in Fig. 6, and second that it has some physical significance, as explained below.

The linear relationship shown in Fig. 7 between σ_1(craze) and $\sigma_e(S_0, \sigma_2)$ establishes a correlation between σ_1 and σ_2 at craze initiation that overcomes the limitations of previous craze criteria. As points A and B fall outside the main scatter band, they have been omitted from the calculation of a linear regression line. The justification for this decision is that Sternstein's data were intended to define a lower bound for visual observation of crazes, and that crazing is inevitably affected by the onset of general plasticity close to the von Mises envelope, so that some high readings are to be expected. Without points A and B, the correlation coefficient is 0.96, and the intercept on the ordinate axis is 0.96 MPa. A straight line drawn parallel to the regression line, but running through the origin, marks the lower bound on the experimental data.

On the basis of this empirical correlation, the criterion for craze formation in specimens containing no obvious cracks or flaws can be written:

$$\sigma_1(\text{craze}) = S_0\left(1 - R + R^2\right)^{0.5} \tag{18}$$

This equation correlates the craze opening stress with a critical local plastic flow stress $S_0(1, R, 0)$ operating somewhere in the specimen when crazing is first observed. It raises two questions, one relating to the location of the controlling plastic zone, and the other to the relatively low effective stresses that are responsible for plastic flow. Under uniaxial tension the critical local flow stress is 24.4 MPa, whereas the global shear yield stress is 41.6 MPa. Nevertheless, there is general agreement that shear yielding at the crack/craze tip always precedes crazing. As the meniscus instability mechanism depends upon some form of relatively rapid flow, something unusual must be happening at the meniscus.

Of the two plastic flow regions that are responsible for craze growth, the craze wall can be discounted as the region in which the critical local tensile stress $\sigma_{1L}(\text{crit}) = S_0$. While the craze is propagating, σ_{1L} is the fibril drawing stress σ_{fd}, which is approximately equal to σ_1(craze) [5]. Only under uniaxial tension is $\sigma_{fd} = S_0$. Plasticity in the craze wall cannot account for the relationship expressed in Eq. (18) and Fig. 7.

Local plasticity is a necessary condition for fibril drawing, and is made possible at moderate local stresses by the enhanced mobility of the chain segments. This might be the result of strain softening as the strain increases from ~0.01 in the sub-surface to >2 in the craze fibrils, but a more likely explanation is that it is due to the close proximity of the craze wall. Numerous studies have shown that the mobility of chain segments increases substantially within 5–10 nm of a free surface, and that this leads to a substantial depression in the glass transition temperature. Further information on this rapidly developing area can be found in a review by Jones [51] and a recent paper by Peter et al. [52], which is quoted to represent a large body of current literature.

The other region of plastic flow is the craze tip. Here again there is a small plastic zone that is within 5 nm of a free surface and is subject to a high strain gradient, from ~0.01 in the

bulk of the specimen to a much higher level in the meniscus. High levels of fluidity would not be possible in the meniscus without enhanced chain segment mobility. The mechanical properties of the polymer forming the meniscus appear to be comparable with those of a non-crystalline thermoplastic at a temperature well above T_g, where it can best be described as elasto-viscous. Elasto-viscous behaviour is responsible for the phenomenon of melt fracture, which occurs in extruder dies at high rates of elongation [53], and there are possible parallels between melt fracture and meniscus instability.

The standard LEFM approach is to treat crazes as Dugdale yield zones, which are modelled by applying closure stresses to reduce the craze tip stress concentration factor to 1.0, then wedge-opening forces to generate enhanced tensile strains at the tip of the yield zone [40,49,50]. This method predicts an elastic stress concentration ahead of the craze tip, where first yield occurs. Closer to the tip, stress relaxation occurs, and the polymer flows under effective stresses that are lower than the macroscopic yield stress. The evidence from Eq. (18) and Fig. 7 indicates that under uniaxial tension the critical effective stress in the meniscus at the point of instability is 24.4 MPa in PMMA at 60 °C.

It is important to remember that meniscus instability is a response to an excessive rate of wall separation [23]. If the fluid cannot flow rapidly enough to maintain stability, it undergoes cohesive failure and forms fibrils. In a craze, the wall separation rate is determined by the fibril drawing stress, which is approximately equal to σ_1(craze) [5]. The flow rate in the meniscus is controlled by the reduced local viscosity associated with enhanced molecular mobility, and by the effective stress applied to the plastic zone. If S_0 remains constant and σ_2 becomes increasingly negative, meniscus instability therefore occurs at a higher rate of wall separation, which is sustained by a corresponding increase in $\sigma_{1\infty}$. This explains the general form of the craze criterion in Figs. 1 and 2. Although fibril drawing and craze tip plastic flow are different processes, both are controlled by shear flow in the fluidized polymer close to a free surface, and depend upon the same Eyring kinetics. Consequently, an increase in critical flow rate at the craze tip is matched by an increase in fibril drawing rate. On the evidence of Sternstein's biaxial data, it can be concluded that the meniscus region is able to support large differences in principal stresses, unlike a true (Newtonian) liquid. In other words, the polymer close to the meniscus behaves as an elasto-viscous material rather than a simple liquid, as discussed earlier.

It is interesting that σ_{1L}(crit), the critical local tensile stress at instability, has the same value S_0 under all applied biaxial stress states. This is one of many areas identified in the present study that would repay further investigation.

Variations in test temperature appear to affect rates of fibril drawing and craze tip yielding equally. Consequently, Eq. (18) defines biaxial yielding over a wide range of temperatures, as observed by Sternstein et al. [1–3]. Only the parameter S_0 changes, as predicted by the Eyring equation. The stress required to reach the critical flow rate decreases with increasing temperature.

6. Discussion

This study has shown that the formation of visible crazes is governed by two quite different criteria. Initiation occurs when the strain energy release rate G_I reaches a critical value, G_I(nasc), which is typically between 0.1 and 1.0 J m^{-2} in glassy thermoplastics. Propagation occurs when the loading conditions are sufficient to induce instability in the resulting craze tip meniscus. The distinction between the two criteria is unimportant when the specimen contains relatively large cracks or notches, because in these cases the condition $G_I > G_{IC}$ is easily satisfied, where typical values for G_{IC} are in the range 100–1000 J m^{-2}. Craze initiation is immediately followed by both craze growth and crack propagation. Dugdale's model predicts the current length of the craze, which increases with crack length [40]. However, G_I(nasc) is so low that crazes can also initiate from microscopic flaws or cracks, which do not necessarily propagate as the craze extends. Under these conditions, the craze propagation criterion becomes important. Its influence is shown most clearly in biaxial tests on apparently defect-free specimens.

There are some parallels here with fatigue crack propagation. Large precracks enable the specimen to reach the critical crack-tip stress intensity K_{IC} during the first loading cycle, so that the finer details of propagation behaviour are unimportant. At the other extreme, very small precracks remain inactive because the stresses required to reach the threshold amplitude for crack growth, ΔK_{th}, are above the shear yield stress. Between these limits, fatigue crack growth is controlled by crack-tip conditions, which are characterized by the stress intensity amplitude ΔK_I, the loading ratio K_I(min)/K_I(max), and a number of other factors including frequency and waveform. Efforts to develop empirical criteria for fatigue failure continued until relatively recently, and were abandoned only when fracture mechanics became generally recognized as the most rational basis for characterizing and predicting sub-critical crack growth. The same comments apply to sub-critical crack growth under static loading. In glassy polymers, slow crack growth under both dynamic and static loadings invariably involves the initiation and propagation of crazes, and is best analyzed using fracture mechanics.

The new criterion for craze initiation proposed in this paper is simply an adaptation of the Griffith equation. The three elements of novelty lie in recognizing that craze initiation should be classed as a type of fracture process rather than a form of yielding, that any criterion for craze initiation must contain a critical flaw size, and that the critical strain energy release rate can be as low as 0.1 J m^{-2}. This low value is consistent with G_{IC} measurements on glassy polymers with low molecular weights, and to a lesser extent with ΔK_{th} data from fatigue tests on the same materials. There are practical problems in detecting crack growth at vanishingly low propagation rates and defining the real threshold. Like fatigue cracks, crazes often initiate from microscopic surface flaws or internal defects. There is ample experimental evidence for craze nucleation at rounded flaws with dimensions below 1 μm, including scratches, embedded dust, and spherical rubber particles.

Kramer attributes variations in crazing resistance between different glassy thermoplastic polymers to differences in the operational surface energy Γ_s, which is higher than the true surface energy given in reference books [47,48]. These differences arise mainly because the formation of craze fibrils necessarily involves breaking chemical bonds, and the number of bonds broken depends upon the entanglement density.

The principles outlined above provide a sound basis for reinterpreting some of the puzzling results that have been reported in the past. Among these are Berry's observations on fracture in PS and PMMA specimens containing introduced cracks of length a_0 [41]. In both materials, the tensile stress at fracture σ_f is proportional to $a_0^{-0.5}$ over a wide range of crack lengths, in accordance with Eq. (9). However, there is a deviation at small a_0. Below a certain limit, the strength no longer increases as the introduced crack length is reduced. Instead, crazes that originate elsewhere in the specimen are responsible for fracture. For PMMA this limit lies at 50 μm, but for PS it is much higher, at 1 mm.

The explanation for the difference is to be found in Berry's photographs, which show the cracks generated in the two polymers on insertion of a wedge into square-tipped saw cuts. The aim was to sharpen the tip while increasing a_0 by a small amount. In PS this procedure resulted in a dense layer of sub-surface crazing close to the extension crack, which raised G_{IC} to 1700 J m^{-2} in subsequent LEFM tests. By contrast, in PMMA the wedge produced a clean crack extension, which presumably had a single craze at its tip; the measured G_{IC} was 300 J m^{-2}. Polystyrene's low intrinsic resistance to craze initiation resulted in an artificially high fracture toughness measurement, so that a stress of 40 MPa was required to fracture a specimen with $a_0 = 1$ mm. By contrast, the tests on PMMA gave a more realistic fracture toughness because there was only one notch-tip craze to absorb the energy, so that a 50 μm crack was sufficient to induce fracture at an applied stress of 40 MPa. In both polymers, each active small flaw initiated a single craze at 40 MPa, and many of them were capable of causing final fracture before G_I became critical for the introduced crack. With care, it is now possible to avoid multiple crazing at the notch tip in polystyrene LEFM specimens, so that the anomaly becomes much less apparent. Even so, it is extremely difficult to reduce the tip radius of an introduced macroscopic crack to 0.25 μm. In that respect, small scratches always have an advantage that can compensate for their small size. The new LEFM criterion explains why they can be so effective in initiating both crazing and final fracture.

7. Conclusions

This study has demonstrated that a coherent theory of craze formation can be constructed on the basis of the established principles of polymer mechanics. A criterion based on fracture mechanics overcomes the difficulties inherent in previous criteria, notably those caused by ignoring small flaws, or treating them as inconvenient geometrical irregularities that pose intractable problems of stress analysis [5].

The answer is to recognize that crazing is essentially a frustrated fracture process, and that the dimensions and geometry of the initiating flaw must be included in any criterion for craze formation. For this reason, attempts to develop criteria based simply on stress invariants can never be successful. Crazing, like brittle fracture but unlike shear yielding, can be suppressed by carefully polishing the surface of the specimen to reduce the flaw size. This observation alone is sufficient to demonstrate that the initiation stage is best modelled using fracture mechanics.

The adventitious flaws responsible for crazing in plain glassy thermoplastics are usually extremely small, with dimensions below 1 μm, so that initiation takes place from what appears to the naked eye to be a perfect surface. The key to understanding the effectiveness of such small flaws is the very low fracture toughness associated with breakdown of the van der Waals bonds in polymeric glasses such as polystyrene and PMMA. Nascent crazes with thicknesses of approximately 10–20 nm form at a critical strain energy release rate $G_{nasc} < 1$ J m^{-2}, whereas final fracture of the craze, at a thickness of ~3000 nm, is characterized by a fracture energy $G_{IC} \sim 300$ J m^{-2}.

This paper has also shown how the von Mises yield criterion can be used in combination with the meniscus instability mechanism to explain the observed dependence of σ_1(craze) on σ_2 in biaxial tests on plain specimens containing no visible cracks or flaws. The reference state is uniaxial tension, where S_0 is both the critical tensile stress σ_1(craze) and the critical local von Mises effective stress required for craze extension, σ_{eL}(crit). Introducing a second principal stress σ_2 changes the effective stress in the craze tip plastic zone, thereby increasing or decreasing the flow rate in the meniscus. To induce meniscus instability, it is necessary to raise or lower the rate of separation of the craze walls, which requires an increase or decrease in σ_1(craze). Analysis of the data on crazing under biaxial loading shows that the critical tensile stress acting on the craze tip plastic zone at instability remains constant at S_0 when the biaxial stress state is varied.

Because of the inconsistencies in previous treatments of craze formation, it has hitherto proved difficult to develop the subject properly as a branch of polymer physics. The new perspective outlined in this paper overcomes these obstacles, and opens up the area to further investigation.

Acknowledgement

The author thanks Professor S.S. Sternstein for stimulating discussions.

References

[1] Sternstein SS, Ongchin L, Silverman A. Appl Polym Symp 1968;7:175.
[2] Sternstein SS, Ongchin L. Polym Prepr Am Chem Soc Div Polym Chem 1969;10:1117.
[3] Sternstein SS, Myers FA. J Macromol Sci Phys 1973;B8:539.
[4] Gearing BP, Anand L. Int J Solids Struct 2004;41:3125.
[5] Donald AM. In: Haward RN, Young RJ, editors. The physics of glassy polymers. 2nd ed. London: Chapman & Hall; 1997.

[6] The term ‘craze thickness’ is used here to denote wall-to-wall distance, on the grounds that the thickness of a layer is its smallest dimension. Some authors call this ‘craze width’, a term that appears to have originated from electron microscopy, where the thickness of the section is usually smaller than the wall-to-wall dimension of the craze.
[7] Argon AS, Salama MM. Philos Mag 1976;36:1217.
[8] Kramer EJ. Polym Eng Sci 1984;24:761.
[9] Lauterwasser BD, Kramer EJ. Philos Mag A 1979;39:1217.
[10] Donald AM, Kramer EJ. J Polym Sci Polym Phys 1982;20:899.
[11] Berger LL. Macromolecules 1990;23:2926.
[12] Plummer CJG, Donald AM. Macromolecules 1990;23:3929.
[13] Krupenkin TN, Fredrickson GH. Macromolecules 1999;32:5029.
[14] Krupenkin TN, Fredrickson GH. Macromolecules 1999;32:5036.
[15] Rottler J, Barsky S, Robbins MO. Phys Rev Lett 2002;89:148304.
[16] Rottler J, Robbins MO. Phys Rev Lett 2002;89:195501.
[17] Rottler J, Robbins MO. Phys Rev E 2003;68:011801.
[18] Basu S, Mahajan D, Van der Giessen E. Polymer 2005;46:750.
[19] Oxborough RJ, Bowden PB. Philos Mag 1973;28:547.
[20] Ward IM. Mechanical properties of solid polymers. 2nd ed. New York: Wiley; 1983.
[21] Ward IM. J Mater Sci 1971;6:1397.
[22] Dugdale DS. J Mech Phys Solids 1960;8:100.
[23] Argon AS, Hannoosh JG. Philos Mag 1977;36:1195.
[24] Bucknall CB. Toughened plastics. London: Applied Science Publishers; 1977.
[25] Sternstein SS, Rosenthal J. In: Deanin RD, Crugnola AM, editors. Toughness and brittleness of polymers. Advances in chemistry series 154. Washington DC: American Chemical Society; 1976.
[26] Argon AS. Pure Appl Chem 1975;43:247.
[27] Maxwell B, Rahm LF. Ind Eng Chem 1949;41:1988.
[28] Bergen RL. SPE J 1962;18:667.
[29] Sternstein SS, editor. Polymeric materials: relationships between structure and mechanical properties. Metals Park, Ohio: American Society of Metals; 1973 [chapter 7].
[30] Kausch HH. Polymer fracture. Berlin: Springer Verlag; 1978.
[31] Kramer EJ. In: Kausch HH, editor. Advances in polymer science, vols. 52–53. Berlin: Springer Verlag; 1983.
[32] Argon AS, Hannoosh JG, Salama MM. Fracture, vol. 1. Waterloo, Canada: ICF4; 19–24 June 1977.
[33] Stroh AN. Proc R Soc London Ser A 1954;223:404.
[34] Bucknall CB, Ayre DS, Dijkstra DJ. Polymer 2000;41:5937.
[35] Bucknall CB, Soares VLP. J Polym Sci Polym Phys 2004;42:2168.
[36] Lazzeri A, Bucknall CB. J Mater Sci 1993;28:6799.
[37] Bucknall CB, Karpodinis A, Zhang XC. J Mater Sci 1994;29:3377.
[38] Bucknall CB. In: Haward RN, Young RJ, editors. The physics of glassy polymers. 2nd ed. London: Chapman & Hall; 1997.
[39] Shull KR, Creton C. J Polym Sci Polym Phys 2004;42:4023.
[40] Williams JG. Fracture mechanics of polymers. London: Ellis Horwood; 1984.
[41] Berry JP. J Polym Sci 1961;50:313.
[42] Drabble F, Haward RN, Johnson W. Br J Appl Phys 1966;17:241.
[43] Michler GH. Colloid Polym Sci 1985;263:462.
[44] Döll W. In: Kausch HH, editor. Advances in polymer science, vols. 52–53. Berlin: Springer Verlag; 1983.
[45] Robertson RE. Polym Prepr Am Chem Soc Div Polym Chem 1974; 34(2):229.
[46] Kusy RP, Turner DT. Polymer 1976;17:161.
[47] Wu S. Polymer interface and adhesion. New York: Marcel Dekker; 1982. p. 88.
[48] Brandrup J, Immergut EH, Grulke EA, Abe A, Block DR. Polymer handbook. 4th ed. New York: Wiley; 2005.
[49] Anderson TL. Fracture mechanics: fundamentals and applications. 3rd ed. Boca Raton, FL: Taylor & Francis; 2004.
[50] Broek D. Elementary engineering fracture mechanics. 4th ed. Dordrecht; 1991.
[51] Jones RAL. In: Haward RN, Young RJ, editors. The physics of glassy polymers. 2nd ed. London: Chapman & Hall; 1997.
[52] Peter S, Meyer H, Baschnagel J. J Polym Sci Polym Phys 2006;44:2951.
[53] Tadmor Z, Gogos CG. Principles of polymer processing. New York: Wiley; 1979.